AN EVALUATION OF FORMATION PROCESSES FOR TRANSVERSE AEOLIAN RIDGES ON MARS.

J. R. Zimbelman[1] and S. H. Williams[2], [1]CEPS/NASM MRC 315, Smithsonian Institution, Washington, D.C. 20013-7012 (zimbelmanj@si.edu), [2]Education/NASM MRC 305, Smithsonian Institution, Washington, D.C. 20013-7012 (williamssh@si.edu).

Introduction: Mars Orbiter Camera (MOC) images have revealed the nearly ubiquitous occurrence of decameter-wavelength-scale ripple-like features on Mars (Fig. 1) [1-3]. These features have been given

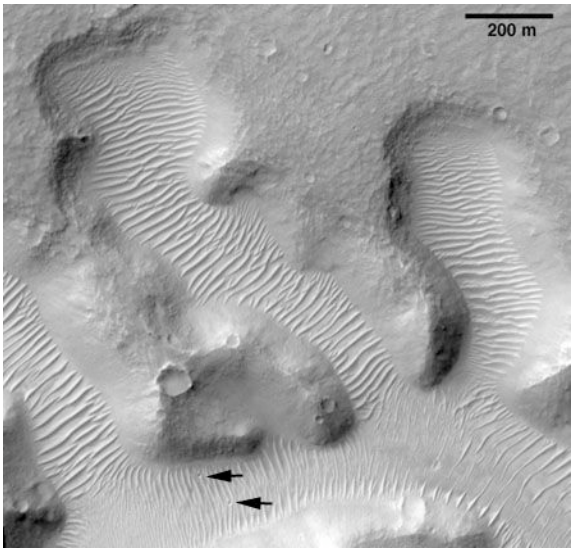

Figure 1. Transverse Aeolian Rigdes (TARs) on the floor of Nirgal Vallis. Arrows indicate impact craters superposed on TARs. Near 27.5° S, 317.2° E. 2.8 m/p, MOC image E02-02651. NASA/JPL/MSSS.

the non-genetic name of "Transverse Aeolian Ridges" (TARs) [4], and are interpreted to be either small sand dunes or large ripples [1-8]. The Mars Exploration Rovers (MERs) Spirit and Opportunity have revealed the presence of both decimeter-wavelength sand ripples and meter-wavelength granule-coated sand-cored ripples at both landing sites [9-12].

Field work investigating granule ripples at sites throughout the western U.S., and particularly at Great Sand Dunes National Park and Preserve (GSDNPP), have documented the physical attributes of these features [13-16], including the first documented rate of movement of granule ripples as induced by the impact of saltating sand [17]. Here we present both the results of the field work, including measured profiles scaled by the wavelength of the features, and compare the terrestrial data to High Resolution Imaging Science Experiment (HiRISE) data [18-19]; specifically, a profile across a TAR from the first publicly released full-resolution HiRISE image [20].

Field results for ripples and dunes: We measured aeolian bedforms at several wavelength scales using different techniques. A shadow cast by a straight edge across both sand ripples and a gnomen allows a single vertical photograph to provide a topographic profile across the ripples with a vertical precision <0.3 mm [21], as shown in Figure 2. The profiles of granule

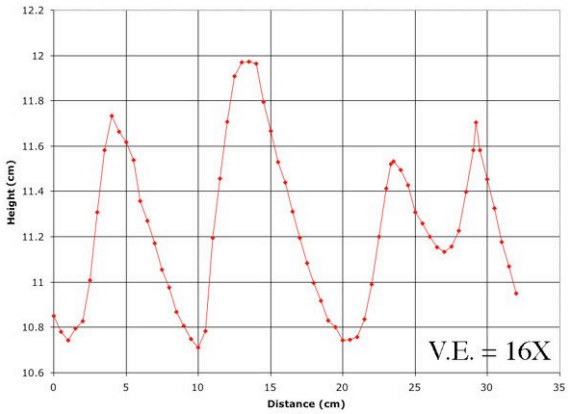

Figure 2. Profile of typical sand ripples. Wind was from the left. Wavelength = 9.8 cm (GSDNPP, CO).

ripples, where grains 1-2 mm in diameter coat a core of medium sand, were measured at 10 cm intervals relative to a laser beam projected above the ripple, providing a topographic profile with a vertical precision of ~0.1 cm (Fig. 3). Granule ripples are the result of

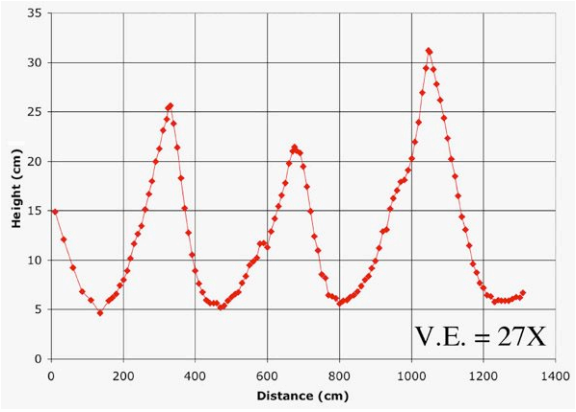

Figure 3. Profile across granule ripples. Wind was from the right. Wavelength = 3.7 m (GSDNPP, CO).

movement of the granules by impact creep resulting from saltating sand [e.g., 22]. Along with fully devel-

oped granule ripples, like those illustrated in Figure 3, we also measured the topography of sand ripples with an incomplete covering of granules, which had the effect of increasing the average wavelength. Large granule ripples have wavelengths comparable to that of small transverse sand dunes, however the particle size on the surface allows the two types of features to be readily separated [23]. For sand dunes, we used Differential Global Positioning System (DGPS) data to obtain topographic profiles with a precision <4 cm [e.g., 24-25] (Fig. 4). By scaling the measured profiles

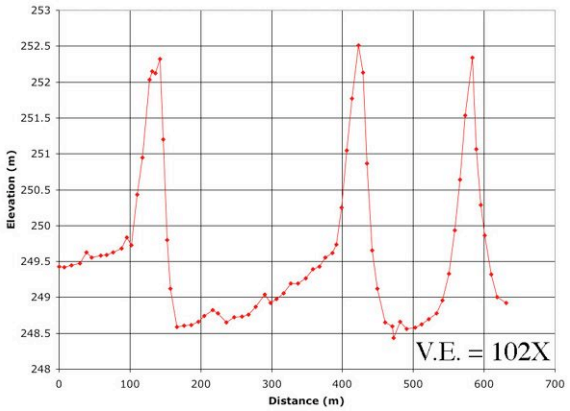

Figure 4. Profile across transverse sand dunes. Wind was from the right. (Rice Valley, CA).

by the average wavelength of the feature, we obtained profiles that show characteristic shapes independent of the size of the feature [14] (Fig. 5). Scaled profiles

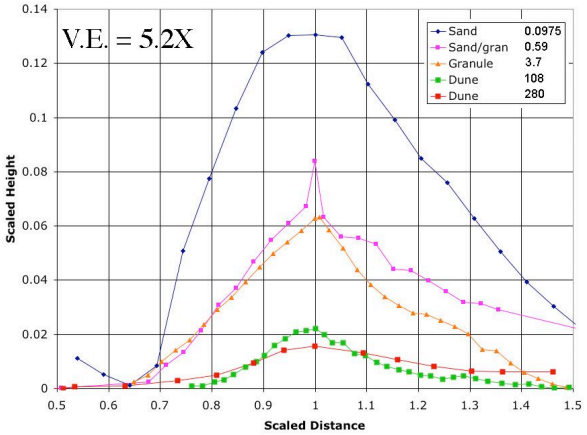

Figure 5. Profiles scaled (in both height and horizontal distance) by the feature wavelength (given in meters, in inset box). Wind is from the left for all profiles. From [14].

provide a means for testing the possible formation mechanism for features observed remotely, as is necessarily the case for features on Mars.

Examining a TAR on Mars: The HiRISE instrument on the Mars Reconnaissance Orbiter is providing the best views of Mars ever obtained from orbit [e.g., 18]. The new images are particularly well suited to study aeolian processes and landforms [e.g., 19]. Here we make use of the first full-resolution HiRISE image released to the public after the conclusion of aerobraking. The image is of the floor of Ius Chasma, which happens to include numerous TARs (Fig. 6).

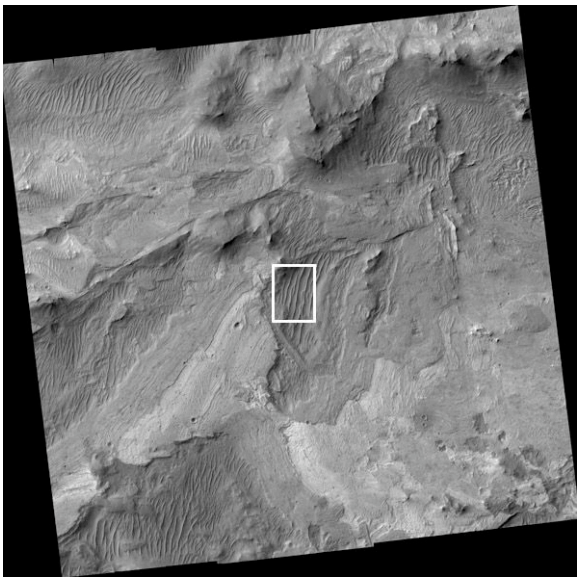

Figure 6. HiRISE image of the floor of Ius Chasma., the first full-resolution (25 cm/p) HiRISE image released to the public [20]. Centered at 7.8° S, 279.5° E. North is up. Box shows location of Figure 7. PIA08792. NASA/JPL/U of A

The central portion of the image shows a field of TARs in great detail. The albedo across the TAR field appears to be very uniform. If we assume that the albedo is indeed precisely uniform across the TAR field, the brightness values along a line perpendicular to the crest of the feature can be converted to a topographic profile through the furthur assumption that the surface behaves in a Lambertian manner (that is, the surface brightness is directly proportional to the cosine of the solar illumination). Through an iterative process, we can assign a value for the brightness that corresponds to a flat horizontal surface; deviations from that value are then converted to a local slope based on the brightness value from the image profile. The result is a rather uniform shape across the TAR (Fig. 8). By measuring the average wavelength across several TARs along the line used for the profile, we obtain an average wavelength of 38.8 m; both the vertical and horizontal distances can then be scaled accordingly (Fig. 9).

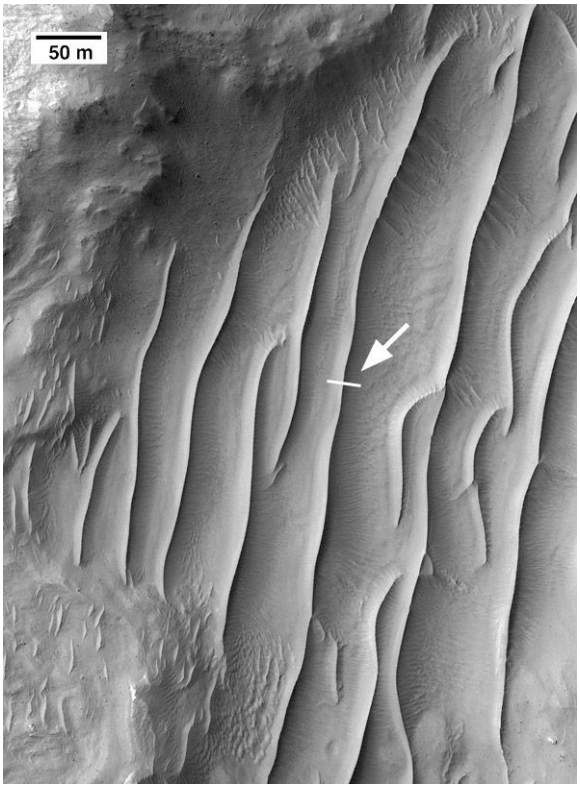

Figure 7. Subscene from HiRISE image in Figure 6. Arrow indicates line for profile shown in Figure 8. NASA/JPL/U of A.

The resulting scaled profile can then be compared to the scaled terrestrial profiles shown in Figure 5.

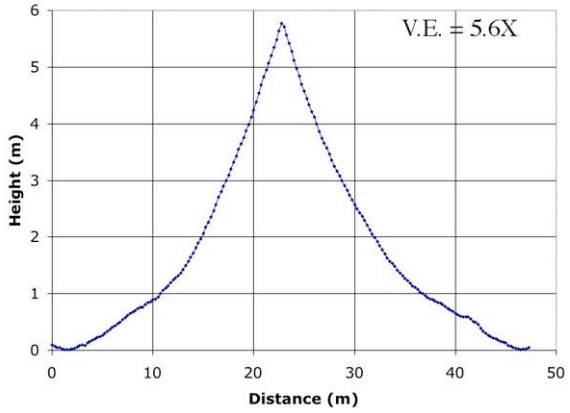

Figure 8. Profile across TAR (line in Figure 7), derived by assuming uniform albedo and Lambertian photometric properties for the surface materials.

Discussion: The very uniform shape of both the raw profile (Fig. 8) and the scaled profile (Fig. 9) across the TAR are clearly unlike both sand ripples (with their asymmetry based on the wind direction, and rounded crest) and the transverse sand dunes (with very low scaled heights). The scaled TAR shape is most similar to that of the granule ripple profile (orange in Fig. 5), and is even relatively similar to granule-coated sand ripples (purple in Fig. 5). However, the scaled height of the TAR is too large by about a factor of three relative to the scaled height of the granule ripple. We are at a loss to explain this height difference, but it may be a consequence of the assumptions made in obtaining the TAR profile, or perhaps the difference in the acceleration of gravity between Earth and Mars (which differ by a factor that is very close to the difference between the scaled heights). We are in the process of making additional profiles across other TARs visible in the same HiRISE image, and we will report those results at the 7th Mars conference. We are optimistic that the technique illustrated here will provide a means for evaluating TARs across Mars, to establish their affinity to sand ripples, granule ripples, or sand dunes, and the very different processes represented by all three bedform types.

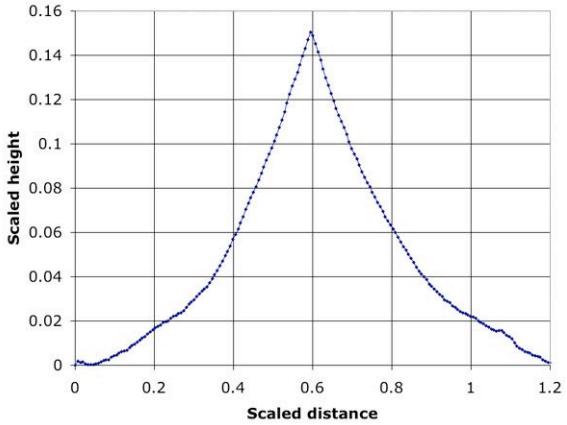

Figure 9. TAR profile (from Figure 8) scaled by the average wavelength of 38.8 m. Comparison with scaled profiles in Figure 5 indicates a shape most similar to that of granule ripples, although the scaled height here is roughly too large by a factor of three.

References: [1] Malin M. C. et al. (1998) *Science, 279*, 1681-1685. [2] Edgett K. S. and Malin M. C. (2000) *JGR, 105*, 1623-1650. [3] Malin M. C. and Edgett K.S. (2001) *JGR, 106*, 23429-23570. [4] Bourke M. C. et al. (2003) *LPS XXXIV*, abstract #2090. [5] Zimbelman J. R. and Wilson S. A. (2002) *LPS XXXIII*, Abstract #1514. [6] Wilson S. A. et al. (2003) *LPS XXXIV*, Abstract #1862. [7] Zimbelman J. R. (2003) *6th Int. Conf. Mars*, Abstract #3028. [8] Wilson S. A. and Zimbelman J. R. (2004) *JGR, 109*, 10.1029/2005JE002247. [9] Squyres S. W. et al. (2004) *Science, 305*, 794-799. [10] Squyres S. W. et al. (2004) *Science, 306*, 1698-1703. [11] Greeley R. et al. (2004) *Science, 305*, 810-821. [12] Sullivan R. et al.

(2005) *Nature, 436*, 10.1038/nature03641. [13] Williams S. H. et al. (2002) *LPS XXXIII*, Abstract #1508. [14] Zimbelman J. R. and Williams S. H. (2005) *Trans. AGU 86(18)*, Abstract P21D-07. [15] Dressing C. D. et al. (2006) *LPS XXXVII*, Abstract #1740. [16] Zimbelman J. R. and Williams S. H. (2006) *LPS XXXVII*, Abstract #2047. [17] Zimbelman J. R. et al. (2007) *LPS XXXVIII*, Abstract #1324. [18] McEwen A. S. et al. (2007) *LPS XXXVIII*, Abstract #2031. [19] Bridges N. T. et al. (2007) *LPS XXXVIII*, Abstract #2098. [20] photojournal.jpl.nasa.gov/catalog/ PIA08792. [21] Werner et al. (1986) *Geology, 14*, 743-745. [22] Sharp R. P. (1963) *J. Geol. 71*, 617-636. [23] Wilson I. G. (1972) *Sediment. 19*, 173-210. [24] Zimbelman J. R. and Johnston A. K. (2001) *NM Mus. Nat. Hist. Sci. Bull., 18*, 131-136. [25] Zimbelman J. R. and Johnston A. K. (2002) *NM Geol. Soc. Guidebook, 53rd Field Conf.*, 121-127.